Inorganica Chimica Acta 376 (2011) 350–357

Contents lists available at ScienceDirect

Inorganica Chimica Acta

journal homepage: www.elsevier.com/locate/ica

Four new copper(II) complexes with *di*-substituted *s*-triazine-based ligands

Jinfeng Chu, Wei Chen, Guangxun Su, Yu-Fei Song *

State Key Laboratory of Chemical Resource Engineering, Beijing University of Chemical Technology, 100029 Beijing, PR China

ARTICLE INFO

Article history:
Received 31 March 2011
Received in revised form 22 June 2011
Accepted 29 June 2011
Available online 7 July 2011

Keywords:
Copper
Triazine
Non-covalent interactions

ABSTRACT

In this paper, two *di*-substituted triazine-based ligands, 6-chloro-*N,N,N′N′*-tetrakis-pyridin-2-ylmethyl-[1,3,5]triazine-2,4-diamine (**L1**), and 6-chloro-*N,N′-bis-pyridin-2-ylmethyl-N,N′*-bis-thiophen-2-ylmethyl-[1,3,5]triazine-2,4-diamine (**L2**), have been prepared. Reaction of $CuCl_2{\cdot}2H_2O$ and $Cu(NO_3)_2{\cdot}3H_2O$ with **L1** and **L2** results in the formation of $[Cu_2Cl_4(\mathbf{L1})]{\cdot}3MeOH$ (compound **1**), $[Cu_4(NO_3)_8(\mathbf{L1})_2]{\cdot}2.07CH_2Cl_2{\cdot}0.93MeOH$ (compound **2**), $[Cu_2Cl_4(\mathbf{L2})_2]$ (compound **3**) and $[Cu(NO_3)_2(\mathbf{L2})]{\cdot}CH_2Cl_2$ (compound **4**), respectively, which have been fully characterized and determined by single-crystal X-ray crystallography, FT-IR, elemental analysis, thermogravimetric measurement and magnetic susceptibility. The dinuclear compound **1** shows strong π–π interactions between the neighboring pyridine rings. The nitrate–π (1,3,5-triazine ring) interaction with the distance of 2.755 Å in compound **2**, is the closest contact reported so far. Compounds **3** and **4** are mononuclear copper(II) compounds, in which none of thiophene rings coordinates with copper(II) ion. In addition, the different orientations of two thiophene rings in compounds **3** and **4** lead to the π–π and CH_2Cl_2–π (thiophene ring) interactions in compound **4**, but not in compound **3**.

1. Introduction

Supramolecular chemistry involves the intelligent utilization of non-covalent interactions and all biological systems are based on these efficient interactions [1–4]. Non-covalent interactions such as hydrogen bonding and π–π interactions, play vital roles in defining supramolecular assemblies both in solution and the solid state, and they have recently been extended to those interactions between electron-rich molecule and an electron-deficient π ring [5–7].

The *s*-triazine ring is a remarkable building block to generate supramolecular interactions [8]. This is closely related to its structural characteristics, which include (1) three nitrogen atoms can give rise to coordination or hydrogen bonds; (2) the electron deficient character of triazine ring allows the formation of a variety of supramolecular interactions that appear to be of great significance for the stabilization of some biological macromolecules [9]. A thorough examination of the literature on the triazine-based supramolecular assemblies indicates that despite the fact that there are a large number of *tri*-substituted compounds have been reported so far [8,10], little attention has been paid to the *di*-substituted triazine derivatives. In this study, 6-chloro-*N,N,N′N′*-tetrakis-pyridin-2-ylmethyl-[1,3,5]triazine-2,4-diamine (**L1**), and 6-chloro-*N,N′*-bis-pyridin-2-ylmethyl-*N,N′*-bis-thiophen-2-ylmethyl-[1,3,5]-triazine-2,4-diamine (**L2**) (see Scheme 1) have been designed with N- and S-coordinating groups and non-coordinating Cl with lone pairs, which offer great opportunities for the formation of non-covalent interactions. The crystal structures of the resulting compounds **1**–**4** feature the anticipated non-covalent interactions, leading to the formation of novel 1D and 2D supramolecular arrays.

2. Experimental

2.1. Materials and general methods

The solvents used in the reactions were dried according to standard procedures. All reactions were performed under an inert atmosphere, under strictly anhydrous conditions. All reagents was purchased from commercial sources and used without further purification. The compound of *di*-(2-picolyl)amine was obtained by reaction of one equivalent of pyridin-2-yl-methylamine and one equivalent of pyridine-2-carbaldehyde in MeOH and further reduced by adding excess amount of $NaBH_4$. The compound pyridin-2-ylmethyl-thiophen-2-ylmethyl-amine was obtained by reaction of one equivalent of pyridin-2-yl-methylamine and one equivalent of thiophene-2-carbaldehyde in MeOH and further reduced by adding excess amount of $NaBH_4$. C, H and N analyses were carried out in Peking University using Vario elemental analysis III instrument. Fourier transform infrared (FT-IR) spectra were recorded on a Bruker Vector 22 infrared spectrometer, using the KBr pellet method. ^1H NMR spectra were recorded on Bruker 400 MHz spectrometers at room temperature. Magnetic susceptibility measurements were performed in the temperature range 2–300 K using a Quantum Design MPMS XL-7 SQUID magnetome

---

* Corresponding author. Tel./fax: +86 10 64431832.
E-mail addresses: songyf@mail.buct.edu.cn, songyufei@hotmail.com (Y.-F. Song).

0020-1693/$ - see front matter © 2011 Elsevier B.V. All rights reserved.
doi:10.1016/j.ica.2011.06.041

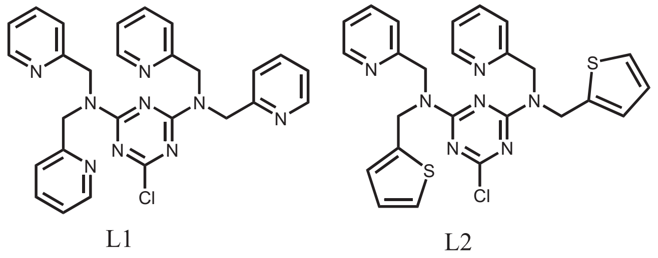

Scheme 1. The molecular structures of 6-chloro-*N,N,N′N′*-tetrakis-pyridin-2-ylmethyl-[1,3,5]triazine-2-4-diamine (**L1**), 6-chloro-*N,N′*-bis-pyridin-2-ylmethyl-*N,N′*-bis-thiophen-2-ylmethyl-[1,3,5]triazine-2,4-diamine (**L2**).

ter equipped with a 7 T magnet. Thermogravimetric (TG) analysis was carried out on a locally produced HCT-2 thermal analysis system in flowing N_2 with a heating rate of 10 °C min^{-1}.

Suitable single-crystals of complexes **1**–**4** were mounted onto the end of a thin glass fiber using Fomblin oil. X-ray diffraction intensity data were measured at 93 K on a Rigaku diffractometer [λ(Mo Kα) = 0.7107 Å]. Structure solution and refinement were carried out with SHELXS-97 [11] and SHELXL-97 [12] via WINGX [13]. Corrections for incident and diffracted beam absorption effects were applied using empirical numerical methods [14]. The weighted *R-factor wR* and goodness of fit S are based on F^2, conventional *R*-factors *R* are based on *F*, with *F* set to zero for negative F^2. The threshold expression of $F^2 > 2\sigma$ is used only for calculating *R*-factors(gt) etc. *R*-factors based on F^2 are statistically about twice as large as those based on *F*, and *R*-factors based on all data will be even larger.

2.2. Ligand synthesis

2.2.1. Synthesis of **L1**

The ligand **L1** was prepared in a similar way to the reported procedure [15]. Yield: 2.88 g (56%). ^1H NMR (400 MHz, *d*-$CDCl_3$, ppm) δ = 4.84 (s, 4H, CH_2), 5.05 (s, 4H, CH_2), 8.54 (d, 2H), 6.92 (d, 2H) 8.43 (d, 2H), 7.66 (t, 2H), 7.20 (s, 4H), 7.18 (t, 2H), 7.05 (t, 2H). IR (KBr, cm^{-1}): 3448(w), 1572(s), 1491(s), 1436(m), 1412(s), 1356(m), 1320(m), 1237(m), 1171(m), 1083(w), 974(w), 947(w), 862(w), 804(w), 761(m), 619(w). *Anal.* Calc. for $C_{27}H_{24}ClN_9$: C, 63.59; H, 4.74; N, 24.72. Found: C, 63.71; H, 4.53; N, 24.47%. EI-MS (positive mode, CH_2Cl_2): $m/z = 510$ $[MH]^+$.

2.2.2. Synthesis of **L2**

2,4,6-Trichloro-[1,3,5]triazine (1.07 g, 5.8 mmol) was dissolved in tetrahydrofurane (50 ml). *N*-Ethyldiisopropylamine (DIPEA) (1.50 g, 11.6 mmol) was added and the mixture was cooled to 0 °C. Then, pyridin-2-ylmethyl-thiophen-2-ylmethyl-amine (2.37 g, 11.6 mmol) was added dropwise in 30 min. After the completion of the addition, the clear reaction mixture was warmed to room temperature and kept at 40 °C for 48 h. Thereafter, the reaction mixture was cooled to 0 °C. *N*-Ethyldiisopropylamine hydrochloride was removed by filtration and the filtrate was concentrated under reduced pressure. The slightly yellow precipitate was isolated on a glass filter and washed with cold ethanol to remove *N*-ethyldiisopropylamine hydrochloride. Yield: 1.84 g (61%). ^1H NMR (400 MHz, *d*-$CDCl_3$, ppm) δ = 4.74 (s, 1H, CH_2), 4.82 (s, 1H, CH_2), 4.93 (s, 1H, CH_2), 4.99 (t, 3H, CH_2), 5.06 (d, 2H, CH_2), 6.79 (t, 1H), 6.86 (t, 1H), 6.93 (t, 1H), 7.02 (t, 1H), 7.22 (t, 1H), 7.64 (t, 1H), 8.55 (t, 1H). IR (KBr, cm^{-1}): 3445(w), 1573(s), 1494(s), 1420(m), 1312(m), 1222(m), 940 (m), 852(w), 798(w), 702(m). *Anal.* Calc. for $C_{25}H_{22}ClN_7S_2$: C, 57.74; H, 4.26; N, 18.85. Found: C, 57.66; H, 4.13; N, 18.57%. EI-MS (positive mode, CH_2Cl_2): $m/z = 519.3$ $[MH]^+$.

2.3. Synthesis of compounds **1**–**4**

2.3.1. Synthesis of compound **1**

A solution of **L1** (70 mg, 0.14 mmol) in MeOH (5 ml) was added dropwise to a solution of $CuCl_2\cdot 2H_2O$ (46 mg, 0.28 mmol) in MeOH (5 ml) and the resulting green solution was left undisturbed at room temperature. Blue crystals suitable for X-ray crystallography were obtained after slow evaporation of the above solution for one week. Yield: 36.0 mg, (30%); IR (KBr, cm^{-1}): 3463(m), 1608(m), 1562(s), 1518(s), 1472(m), 1435(m), 1407(m), 1351(s), 1307(m), 1217(m), 1145(m), 1031(m), 839(w), 807(w), 761(w), 733(m). *Anal.* Calc. for $C_{30}H_{36}Cl_5Cu_2N_9O_3$: C, 41.18; H, 4.15; N, 14.41. Found: C, 41.33; H, 4.26; N, 14.17%.

2.3.2. Synthesis of compound **2**

A solution of **L1** (50.0 mg, 0.09 mmol) in CH_2Cl_2 (5 ml) was added dropwise to a solution of $Cu(NO_3)_{2\text{€}}\cdot 3H_2O$ (46.5 mg, 0.19 mmol) in MeOH (5 ml) and the resulting green solution was left undisturbed at room temperature. Blue-green crystals suitable for X-ray crystallography were obtained after slow evaporation of the above solution for 1 week. Yield: 29.3 mg, (32%); IR (KBr, cm^{-1}): 3445(m), 3069(w), 2962(w), 1611(s), 1569(s), 1517(s), 1487(s), 1386(s), 1282(s), 1223(s), 1155(s), 1106(m), 1018(w), 976(w), 867(w), 809(w), 766(m), 649(w). *Anal.* Calc. for $C_{57}H_{54.86}Cl_{7.14}Cu_4N_{26}O_{24.42}$: C, 34.19; H, 2.76; N, 18.19. Found: C, 34.28; H, 2.99; N, 17.92%.

2.3.3. Synthesis of compound **3**

A solution of **L2** (50 mg, 0.09 mmol) in CH_2Cl_2 (5 ml) was added to a solution of $CuCl_2\cdot 2H_2O$ (28 mg, 0.19 mmol) in MeOH (5 ml) and the resulting solution was filtered and left undisturbed at room temperature. Deep blue crystals suitable for X-ray crystallographic measurement were obtained after five days. Yield: 29.1 mg, (46%); IR (KBr, cm^{-1}): 3451(m), 2924(w), 1659(w), 1609(m), 1562(s), 1522(s), 1473(m), 1442(m), 1406(m), 1350(s), 1289(m), 1253(w), 1218(m), 1152(m), 1108(w), 1057(w), 980(w), 869(w), 840(w), 809(w), 768(m), 729(w), 655(w). *Anal.* Calc. for $C_{25}H_{22}Cl_3CuN_7S_2$: C, 45.88; H, 3.39; N, 14.98. Found: C, 45.52; H, 3.47; N, 14.72%.

2.3.4. Synthesis of compound **4**

A solution of **L2** (50 mg, 0.09 mmol) in CH_2Cl_2 (5 ml) was added dropwise to a solution of $Cu(NO_3)_2\cdot 3H_2O$ (46 mg, 0.19 mmol) in MeOH (5 ml) and the resulting green solution was left undisturbed at room temperature. Blue-green crystals suitable for X-ray crystallography were obtained after slow evaporation of the above solution for 2 weeks. Yield: 30.5 mg, (40%); IR (KBr, cm^{-1}): 3444(w), 3073(w), 2943(w), 1609(s), 1556(s), 1500(s), 1383(s), 1322(s), 1286(s), 1223(s), 1177(m), 1131(m), 1104(m), 1060(w), 1035(m), 1005(s), 966(m), 933(w), 861(m), 833(m), 801(m), 765(m), 709(s), 654(w), 626(w). *Anal.* Calc. for $C_{26}H_{24}CuN_9Cl_3O_6S_2$: C, 39.40; H, 3.05; N, 15.91. Found: C, 39.71; H, 3.43; N 15.42%.

3. Results and discussion

Both ligands **L1** and **L2** were prepared in relatively good yields by reaction of one equivalent of cyanuric chloride and two equivalents of *di*-(2-picolyl)amine or pyridin-2-ylmethyl-thiophen-2-ylmethylamine at 40 °C for 48 h, which resulted in the formation of **L1** in 56% and **L2** in 61% yield, respectively [15].

Compounds **1**–**4** were prepared by the treatment of the corresponding metal salts with **L1** or **L2** at room temperature. The molecular structures and unusual supramolecular characteristics of **1**–**4** are shown in Figs. 1–5. The crystallographic data of **1**–**4**

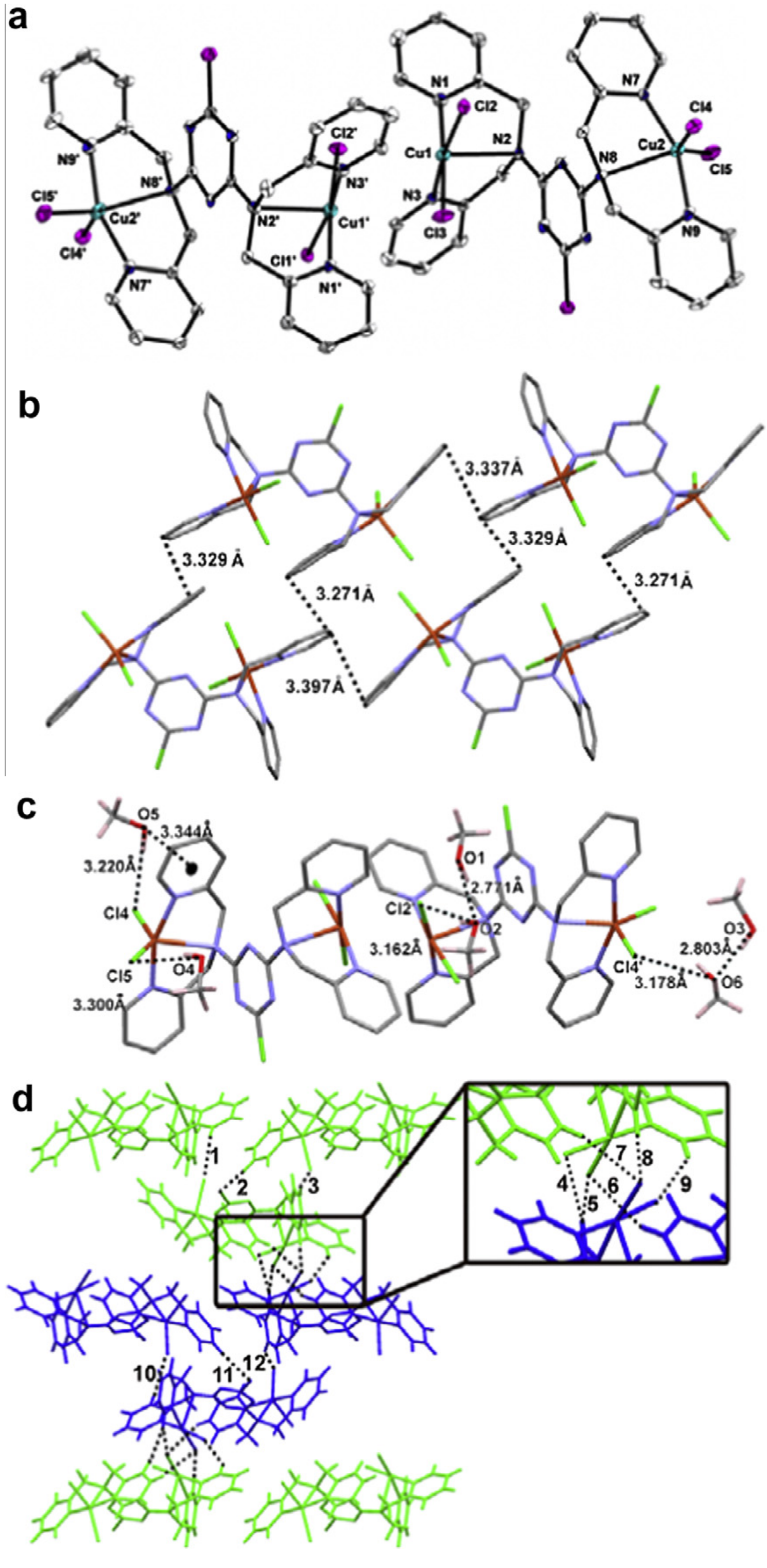

Fig. 1. (a) The crystal structure of **1** with the atoms labeling; hydrogen atoms and solvent molecules have been omitted for clarity. (b) π–π interactions between the neighboring pyridine rings. (c) The hydrogen bonds between methanol oxygens and the coordinated chlorides, and between two neighboring methanol molecules; CH_3OH–π interaction between the methanol molecule and the neighboring pyridine ring in **1**. (d) The crystal packing shows the pyridyl-H···Cl weak hydrogen bonds (dashed lines) of **1**.

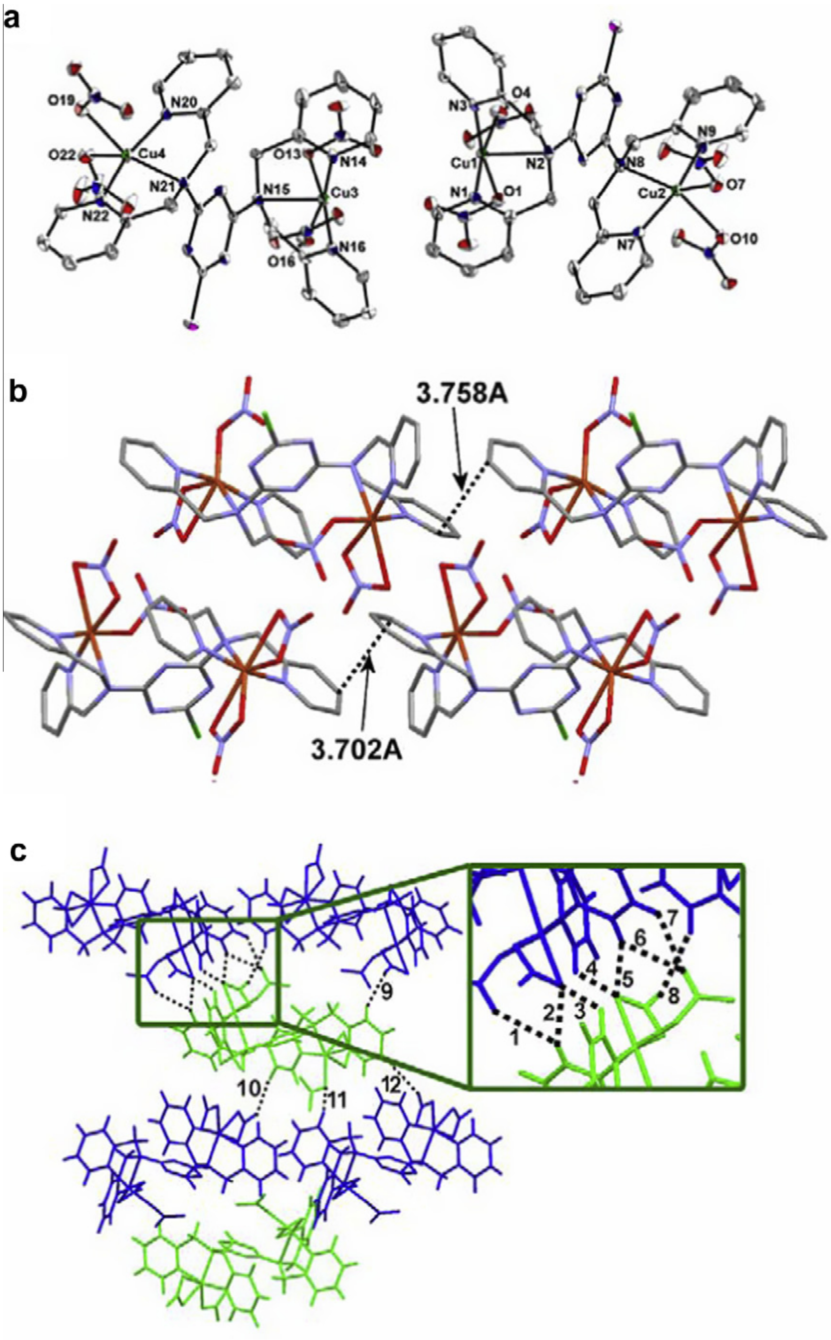

Fig. 2. (a) The crystal structure of **2** with atom labeling; hydrogen atoms and solvent molecules have been omitted for clarity. (b) The crystal packing shows the π-stacking of the pyridyl moieties through the structure viewed along the crystallographic *a* axis with 2-D nature. (c) The crystal packing shows the pyridyl-H···O–nitrate weak hydrogen bonds (dashed lines) of **2**.

have been summarized in Table 1 and the selected bond lengths are listed in Table 2.

3.1. Compound 1

The crystal structure of **1** with the molecular formula of $[Cu_4Cl_8(\mathbf{L1})_2]\cdot 6MeOH$ is illustrated in Fig. 1a. The asymmetric unit contains two dinuclear copper(II) compounds. Each copper(II) ion is coordinated by three nitrogens from dipicolylamine unit of **L1** and two chloride anions with a CuN_3Cl_2 donor set. The pentacoordination of Cu(1) can be best described as distorted square pyramidal with the axial position occupied by the N(2) from a dipicolylamine unit of the **L1** ($\tau = 0.08$, where τ is 0 and 1 for the perfect square pyramidal and trigonal pyramidal geometries, respectively) [16]. The bond angles in the basal plane range from 87.38(11)° to 177.28(12)°, indicating the distortion generated by the semicoordination of the N(2) atom with the Cu(1)–N(2) bond length of 2.6422(37) Å. The coordination of Cu(2) can be described as a distorted trigonal bipyramid geometry ($\tau = 0.33$) with two pyridine nitrogens occupying the axial positions at normal distances and the bond angle of N(7)–Cu(2)–N(9) 158.98(15)°. The Cu–N and Cu–Cl distances are in the range of 1.965(4)–2.409(4) Å, and 2.2741(12)–2.2972(12) Å, respectively. The in-plane angles vary from 98.23(9)° to 139.36(5)°, away from the ideal angle of 120°

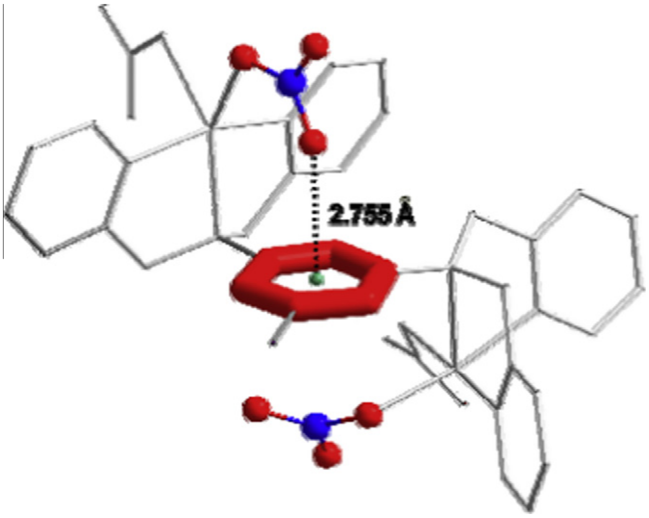

Fig. 3. The oxygen–π interaction between the coordinated nitrate anions and the *s*-triazine rings in **2**.

for a perfect trigonal bipyramid geometry of a copper(II) ion. Two copper(II) ions in the dinuclear complex are in the distance of 7.2324(1) or 7.2212(1) Å in the asymmetric unit.

It is noted that strong π–π interactions could be observed between the neighboring pyridine rings with the C–C distances of 3.329, 3.271, 3.397 and 3.337 Å, and the dihedral angles of 16.40°, 12.08°, 22.23° and 20.24°, respectively (Fig. 1b). As shown in Fig. 1c, hydrogen bonds exist between two neighboring methanol molecules with the bond lengths of O–H···O of 2.771 and 2.803 Å, and between methanol oxygens and the coordinated Cl with the bond distance of O–H···Cl in the range of 3.162–3.300 Å. Furthermore, CH_3OH–π interactions could be observed with the distance of 3.344 Å between the methanol oxygens and the centroid of the pyridine rings in **1**, which might be a consequence of the attractive interaction. The crystal packing of **1** shows weak hydrogen bonds of pyridyl-H···Cl between two adjacent interlayers with C–H···Cl bond distances ranging from 3.431 to 3.698 Å, and bond angles of 132.86–162.02° (Fig. 1d), respectively.

*3.2. Compound **2***

The reaction of one equivalent of **L1** with two equivalents of $Cu(NO_3)_2{\cdot}3H_2O$ yields a dinuclear copper complex of **2**. A molecular plot of the crystal structure of **2** without including the lattice solvent molecules is shown in Fig. 2a. Two dinuclear copper(II) complexes in the asymmetric unit of compound **2** show slight different bond lengths and bond angles. The copper(II) ions are chelated by three nitrogens from dipicolylamine moiety of **L1** and two nitrate ions, which results in a CuO_2N_3 coordination environment. The pentacoordination of Cu(1) can be best described as distorted square pyramidal with the axial position occupied by the N(2) from a dipicolylamine unit (τ = 0.01) [16]. The bond angles in the basal plane range from 84.80(13)° to 171.51(13)°, reflecting the distortion generated by the semicoordination of the N(2) atom (Cu(1)–N(2) distance of 2.4766(3) Å). The coordination of Cu(2) can be described as a distorted trigonal bipyramid geometry (τ = 0.36) with two pyridine nitrogen atoms occupying the axial positions (N(7)–Cu(2)–N(9) = 163.10(15)°). The Cu–N and Cu–O bond lengths are in the range of 1.947(4)–2.153(3) Å, and 2.078(3)–2.132(3) Å, respectively. The in-plane angles vary from 80.72(11)° to 141.74(12)°, away from the ideal angle of 120° for a perfect trigonal bipyramid geometry. The coordination environments of Cu(3) and Cu(4) are similar to those of Cu(1)and Cu(2), respectively. Two copper(II) ions are in the distance of 6.5997(7) or 6.6900(7) Å. As shown in Fig. 2b, π–π interactions between two adjacent pyridine rings could be observed with the C–C distances of 3.702 or 3.758 Å, and the dihedral angles of 17.303° or 18.882°, respectively. Moreover, the crystal packing shows the pyridyl-H···O-nitrate weak hydrogen bonds of **2** with the C–H···O bond lengths in the range of 3.072–3.372 Å, and bond angles 111.24–159.88° (Fig. 2c), respectively.

Interestingly, the oxygen atom in one of the coordinated nitrate anions resides just above the triazine ring (Fig. 3) with the distance of 2.755 Å between the nitrate oxygen and the centroid of triazine ring. The angle of the nitrate oxygen···centroid axis to the plane of the triazine ring is 83.82°, providing proof that the oxygen atom is located perfectly on the triazine moiety. A comprehensive examination of all crystal structures deposited in the Cambridge Structural Database reveals that 21 chloride–π close contacts and 359 nitrate–π close contacts could be found in the pyridine rings in the solid-state structures, and only 3 chloride–π close contacts and 10 nitrate–π close contacts have been found in terms of 1,3,5-triazine ring (Table 3). To the best of our knowledge the nitrate–π interaction with the distance of 2.755 Å in compound **2** represents the closest contact reported so far.

*3.3. Compounds **3** and **4***

The reaction of one equivalent of **L2** and two equivalents of $CuCl_2$ and $Cu(NO_3)_2$ results in the formation of compound **3** and **4**, respectively. The molecular structure of the asymmetric unit of

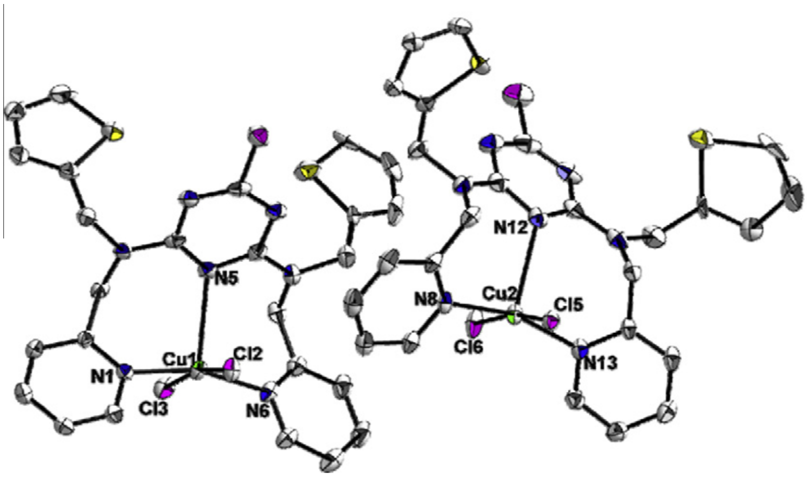

Fig. 4. The crystal structure of **3** shows the mononuclear copper complex in the asymmetric unit; hydrogen atoms have been omitted for clarity.

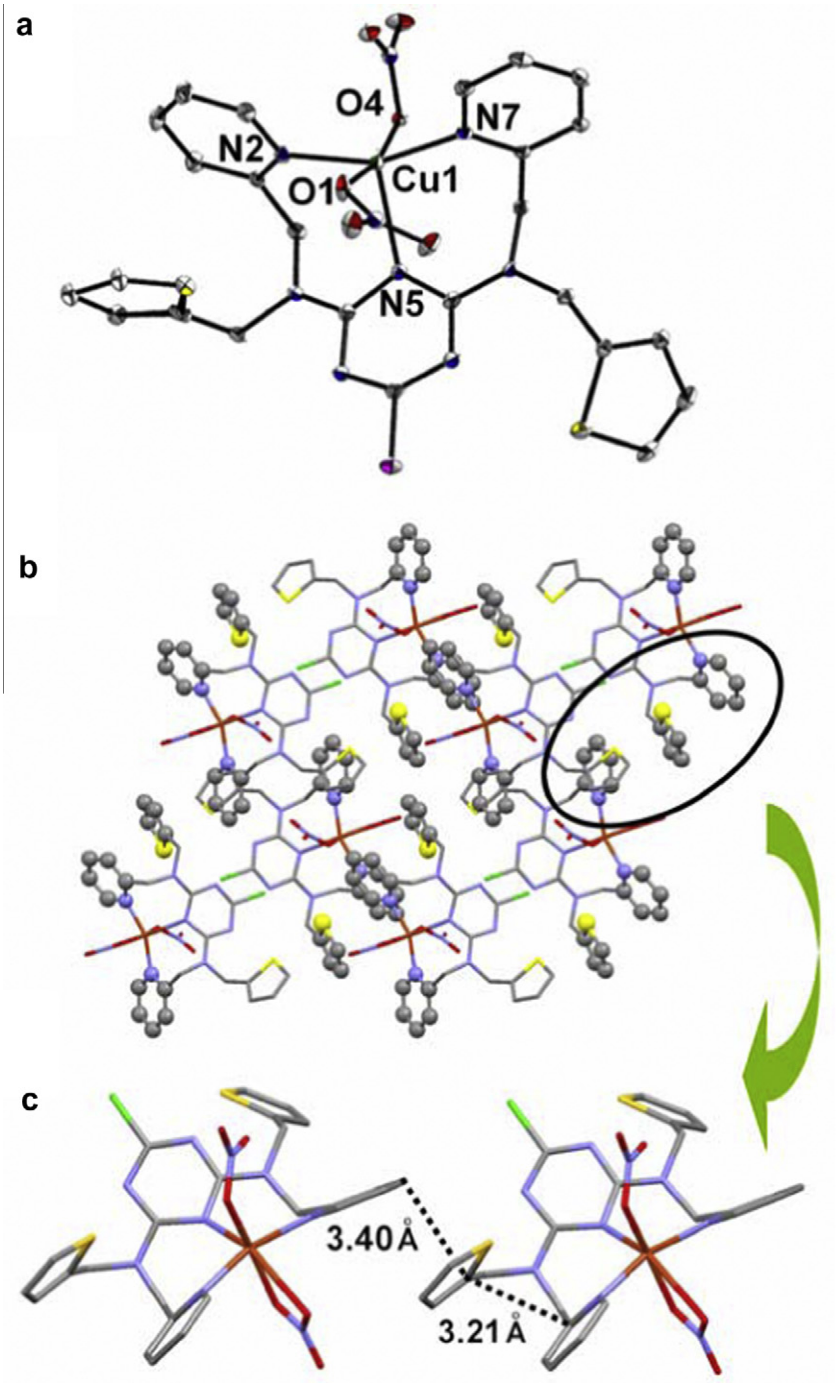

Fig. 5. (a) The crystal structure of **4** shows the mononuclear Cu(II) compound with the atom labeling; hydrogen atoms and dichloromethane solvent molecules have been omitted for clarity. (b) and (c) are the crystal packing of **4**, showing the π–π interactions between the pyridine rings and thiophene rings.

compound **3** contains two mononuclear copper compound, in which the copper(II) ion is coordinated by two pyridine nitrogens, one nitrogen from the triazine unit and two chloride anions (Fig. 4). As such, the copper ion shows a N_3Cl_2 square pyramidal coordination environment with $\tau = 0.10$. A molecular plot of mononuclear compound **4** without lattice solvent molecules is shown in Fig. 5a, in which Cu(1) is coordinated by two nitrate oxygens, two pyridine nitrogens and one nitrogen from the triazine ring with a CuN_3O_2 donor set. Additionally, we have observed the solvent–π interactions between CH_2Cl_2 molecules and the electron-deficient thiophene rings with the Cl^-–π distance of 3.449 Å (Fig. S1). To the best of our knowledge, the interactions between neutral molecules and five-membered rings such as thiophene rings are far more less investigated compared with those of six-membered rings. It should be pointed out that (1) none of the thiophene rings coordinates with copper ions in both compounds **3** and **4**; (2) two thiophene rings in compound **3** appear in clockwise orientation, whereas those in compound **4** in counterclockwise orientation. As a result, the π–π interactions between the neighboring pyridine rings and thiophene rings (Fig. 5b and c) and the CH_2Cl_2–π (thiophene ring) interactions are only observed in **4**, but not in **3**.

3.4. FT-IR spectroscopy

FT-IR spectroscopy results (Fig. S2) indicate that the C=N stretching vibrations of pyridine rings appear at 1571 and

Table 1
Crystallographic data and refinement details for **1**–**4**.

Compounds	**1**	**2**	**3**	**4**
Empirical formula	$C_{30}H_{36}Cl_{15}Cu_2N_9O_3$	$C_{57}H_{54.86}Cl_{7.14}Cu_4N_{26}O_{24.42}$	$C_{50}H_{44}Cl_6Cu_2N_{14}S_4$	$C_{26}H_{24}Cl_3CuN_9O_6S_2$
Formula weight	875.01	2002.34	1309.02	792.55
Crystal system	monoclinic	monoclinic	triclinic	triclinic
Space group	P2(1)	P2(1)	P-1	P-1
a (Å)	10.8152(14)	10.6939(14)	10.3896(11)	11.255(2)
b (Å)	13.8418(18)	29.458(4)	15.9031(15)	11.3310(19)
c (Å)	24.269(3)	13.5972(18)	18.583(2)	13.383(3)
α (°)	90	90	113.575(3)	98.630(2)
β (°)	93.495(2)	111.917(2)	93.461(6)	109.170(2)
γ (°)	90	90	97.040(5)	92.626(2)
V (Å^3)	3626.3(8)	3973.9(9)	2772.6(5)	1585.6(5)
Z	4	4	4	2
Temperature (K)	93(2)	93(2)	93(2)	93(2)
D_{calc} (g cm^{-3})	1.603	1.673	1.568	1.660
μ (cm^{-1})	1.587	1.387	1.257	1.131
Total reflections	29 503	32 273	16 622	11 948
Independent reflections	15 774	16 615	10 253	6351
GOF	0.998	1	0.999	1
R_1 ($I > 2\sigma(I)$)	0.0463	0.0426	0.0435	0.0346
wR_2 ($I > 2\sigma(I)$	0.1024	0.1044	0.0988	0.0737
R_1 (all data)	0.0511	0.0456	0.0546	0.0394
wR_2 (all data)	0.106	0.1077	0.1069	0.0764

Table 2
Selective bond lengths (Å) of Compounds **1**–**4**.

Compound **1**	Cu(1)–N(1)	2.021(4)	Cu(1)–N(3)	2.059(4)	Cu(1)–Cl(2)	2.2623(12)
	Cu(1)–Cl(3)	2.2666(12)	Cu(2)–N(7)	1.965(4)	Cu(2)–N(9)	1.976(4)
	Cu(2)–Cl(5)	2.2741(12)	Cu(2)–N(8)	2.409(4)	Cu(2)–Cl(4)	2.2972(12)
Compound **2**	Cu(1)–O(4)	1.976(3)	Cu(1)–O(1)	1.980(3)	Cu(1)–N(3)	1.991(3)
	Cu(1)–N(1)	2.008(3)	Cu(1)–N(2)	2.477(3)	Cu(2)–N(9)	1.947(4)
	Cu(2)–N(7)	1.956(3)	Cu(2)–O(7)	2.078(3)	Cu(2)–O(10)	2.132(3)
	Cu(2)–N(8)	2.153(3)				
Compound **3**	Cu(1)–N(6)	2.016(3)	Cu(1)–N(1)	2.022(2)	Cu(1)–Cl(2)	2.2581(8)
	Cu(1)–Cl(3)	2.2753(8)	Cu(1)–N(5)	2.579(2)	Cu(2)–N(8)	2.004(3)
	Cu(2)–N(13)	2.023(3)	Cu(2)–Cl(6)	2.2503(8)	Cu(2)–Cl(5)	2.3057(8)
	Cu(2)–N(12)	2.593(2)				
Compound **4**	Cu(1)–O(1)	1.9792(15)	Cu(1)–N(7)	1.9935(18)	Cu(1)–N(2)	2.0033(17)
	Cu(1)–O(4)	2.0151(14)	Cu(1)–N(5)	2.3895(18)		

Table 3
Cl^-–π and NO_3^-–π close contact in CSD.

Close contacts (six-member ring)	Ring	Number of anion–π contacts observed	Mean anion centroid distance (*D*, Å)	Relative standard deviation of the data set (RSD,%)
Cl–π	1,3,5-triazine	3	3.332	n.a.
	pyridine	21	3.427	3
NO_3^-–π	1,3,5-triazine	10	3.160	6.5
	pyridine	359	3.302	4

n.a. stands for "not available".

1491 cm^{-1} in **L1**, which shift to 1563 and 1523 cm^{-1} in **1**, 1566 and 1517 cm^{-1} in **2**, respectively. The above results reveal the coordination of **L1** with copper(II) ions. In terms of **L2**, the C═N stretching vibrations of pyridine rings could be observed at 1571 and 1493 cm^{-1}, which shift to 1563 and 1523 cm^{-1} in **3**, 1558 and 1506 cm^{-1} in **4** after coordination with copper(II) ions. Furthermore, the bending vibrations of pyridine rings of **L1** and **L2** appear at 971 and 972 cm^{-1}, while the corresponding vibrations shift to 979, 977, 980, 960 cm^{-1} in **1–4**, respectively.

3.5. Magnetic susceptibility measurements

Magnetic susceptibility measurements have been performed on the crystalline powders of **1** and **2** at 0.1 Tesla in the range of 6 2–300 K. The plot of χT versus the T [with χ being the magnetization per copper(II) ion] is illustrated in Fig. S3. At 300 K, $\chi T = 0.83$ for **1** and 0.88 cm^3 K mol^{-1} for **2**, respectively, which are very close to the expected values for two uncoupled copper(II) ions ($T = 0.84$ cm^3 K mol^{-1} for paramagnetic systems). The value of χT does not change upon cooling to 9 K, suggesting there are no interactions between copper(II) ions. After that, it starts to decrease and reaches to 0.53 cm^3 K mol^{-1} for **1** and 0.79 cm^3 K mol^{-1} for **2** at 2 K, respectively.

3.6. TG studies

As shown in Fig. S4, the TG results of **1** confirm the initial weight loss of about 10%, corresponding to the loss of MeOH before 200 °C. With the increase of temperature, **1** starts to decompose from 250 °C. Compound **2** shows the first well defined event associated with CH_2Cl_2 and MeOH loss of ca. 10% before 190°, and then **2** starts to decompose. Compound **3** starts to decompose at ca. 300 °C. Compound **4** shows a series of events with the initial weight loss of CH_2Cl_2 ca.10% before 200 °C, which is followed by the decomposition of compound **4** directly.

4. Conclusions

In summary, the deliberate design of *di*-substituted triazine-based ligands of **L1** and **L2** exerts a profound influence on the supramolecular interactions of the resulting crystal structures of compounds **1**–**4**. The dinuclear compound **1** shows strong π–π and hydrogen bonding interactions. The nitrate anion–π interactions with the closest contact of 2.755 Å could be observed in **2**. In the case of compounds **3** and **4**, none of the thiophene rings coordinates with the copper(II) ion, and two thiophene rings are in a clockwise orientation in compound **3**, whereas those in compound **4** are in a counterclockwise orientation. As a result, π–π interactions between the adjacent pyridine rings and thiophene rings are observed only in **4**, but not in **3**. It can be concluded that such non-covalent interactions play significant roles in the formation of interesting supramolecular architectures of **1**–**4**. Further exploration of such interactions for specific application is underway in our lab.

Acknowledgments

The work was supported financially by the National Science Foundation of China (21076020 and 20801003) and the Program for New Century Excellent Talents of Ministry of Education of China (NCET-09-0201) and Beijing Nova Program (2009B12). We also thank Dr. J.K. Tang for his help with the magnetic measurements.

Appendix A. Supplementary material

CCDC 774699, 774700, 774702, and 774703 contains the supplementary crystallographic data for this paper. These data can be obtained free of charge from The Cambridge Crystallographic Data Centre via www.ccdc.cam.ac.uk/data_request/cif. Supplementary data associated with this article can be found, in the online version, at doi:10.1016/j.ica.2011.06.041.

References

[1] (a) G.A. Jeffrey, An Introduction of Hydrogen Bonding, Oxford University Press, Oxford, 1997;
[b] J.W. Steed, J.L. Atwood, Supramolecular Chemistry, John Wiley & Sons, Ltd., Chichester, 2000.
[2] H.J. Schneider, Angew. Chem., Int. Ed. 48 (2009) 3924.
[3] J.W. Steed, D.R. Turner, K.J. Wallace, Chichester, Core Concepts in Supramolecular Chemistry and Nanochemistry, Wiley, Chichester, 2007.
[4] J.C. Ma, D.A. Dougherty, Chem. Rev. 97 (1997) 1303.
[5] E.A. Meyer, R.K. Castellano, F. Diederich, Angew. Chem., Int. Ed. 42 (2003) 1210.
[6] (a) B.L. Schottel, H.T. Chifotides, K.R. Dunbar, Chem. Soc. Rev. 37 (2008) 68;
(b) I. Alkorta, I. Rozas, J. Elguero, J. Am. Chem. Soc. 124 (2002) 8593;
(c) D. Qui_onero, C. Garau, C. Rotger, A. Frontera, P. Ballester, A. Costa, P.M. Dey, Angew. Chem., Int. Ed. 42 (2002) 3389;
(d) M. Mascal, A. Armstrong, M.D. Bartberger, J. Am. Chem. Soc. 124 (2002) 6274.
[7] (a) V. Gorteau, G. Bollot, J. Mareda, A. Perez-Velasco, S. Matile, J. Am. Chem. Soc. 128 (2006) 14788;
(b) A. Perez-Velasco, V. Gorteau, S. Matile, Angew. Chem., Int. Ed. 47 (2008) 921;
(c) R.E. Dawson, A. Hennig, D.P. Weimann, D. Emery, V. Ravikumar, J. Montenegro, T. Takeuchi, S. Gabutti, M. Mayor, J. Mareda, C.A. Schalley, S. Matile, Nature Chem. 2 (2010) 533.
[8] (a) T.J. Mooibroek, P. Gamez, J. Reedijk, Cryst. Eng. Comm. 10 (2008) 1501;
(b) T.J. Mooibroek, P. Gamez, J. Reedijk, Acc. Chem. Res. 40 (2007) 435;
(c) C. Silien, M.T. Raisanen, M. Buck, Angew. Chem., Int. Ed. 48 (2009) 3349.
[9] (a) J.C. Calabrese, D.B. Jordan, A. Boodhoo, S. Sariaslani, T. Vannelli, Biohemistry 43 (2004) 11403;
(b) E.J. Stollar, J.L. Gelpi, S. Velankar, A. Golovin, M. Orozco, B.F. Luisi, Proteins. 57 (2004) 1.
[10] (a) Z. Ahmed, K. Iftikhar, Inorg. Chem. Commun. 13 (2010) 1253;
(b) M. Trivedi, D.S. Pandey, R.Q. Zou, Q. Xu, Inorg. Chem. Commun. 11 (2008) 526;
(c) E.A. Medlycott, G.S. Hanan, Inorg. Chem. Commun. 10 (2007) 229;
(d) S. Demeshko, S. Dechert, F. Meyer, J. Am. Chem. Soc. 126 (2004) 4508;
(e) S. Samaritani, G. Signore, C. Malanga, R. Menicagli, Tetrahedron 61 (2005) 4475;
(f) G. Yua, C. Liu, G. Li, J. Wang, X. Jian, Thermochim. Acta 514 (2011) 51.
[11] G.M. Sheldrick, SHELXS-97, Program for crystal structure solution, University of Göttingen, Germany, 1997.
[12] G.M. Sheldrick, SHELXL-97, Program for crystal structure refinement, University of Göttingen, Germany, 1997.
[13] L.J. Farrugia, J. Appl. Crystallogr. 32 (1999) 837.
[14] R.H. Blessing, Acta Crystallogr., Sect. A. 51 (1995) 33.
[15] D. Vomasta, M. Zabel, B. König, Molbank (2007) M556.
[16] A.W. Addison, T.N. Rao, J. Reedijk, J.V. Rijn, G.C. Verschoor, J. Chem. Soc., Dalton Trans. (1984) 1349.